

Design and Performance of Reinforced Concrete Water Chlorination Tank Totally Reinforced with GFRP Bars: Case Study

Hamdy M. Mohamed¹ and Brahim Benmokrane²

Abstract: Reinforced-concrete (RC) tanks in water and wastewater treatment plants (WWTPs) experience severe corrosion problems resulting from the application of specific treatment methods or chemicals. Municipalities around the world spend hundreds of millions of dollars annually to replace and repair corroded RC tanks. Designing these tanks requires attention not only to strength requirements, but also to durability and crack control. This paper presents the design procedures, construction details, leakage testing, and monitoring results for the world's first RC water chlorination tank totally reinforced with glass-fiber-reinforced polymer (GFRP) bars. The project is located in Thetford Mines, Quebec, Canada. The tank is considered one of the most important components in the city's new water treatment plant. The tank has a volume of over 2,500 m³ and its walls are 4,650 mm high. The foundation, vertical walls, and cover slab were totally reinforced with GFRP bars. The tank was designed to satisfy the serviceability and strength criteria in CAN/CSA S806-12 (CSA 2012), ACI 440.1R-06 (ACI 2006), and ACI 350/350R-06. The tank is fully instrumented at critical locations with fiber-optic sensors to collect strain data. Site inspection showed that the tank performed very well and was able to withstand applied loads without problems or leaking during the leakage test and after eight months under the service condition. DOI: 10.1061/(ASCE)CC.1943-5614.0000429. © 2013 American Society of Civil Engineers.

Author keywords: Fiber-reinforced polymer (FRP) bars; Design; Field applications; Implementation; Water tank; Construction.

Introduction

Conventionally reinforced concrete (RC) tanks have been used extensively in municipal and industrial facilities for water and wastewater treatment plants (WWTPs) for decades. There are three kinds of water tanks: on ground, underground, and elevated. The most commonly used at WWTPs is the underground tank. The tank walls are subjected to lateral pressure from the water and earth, while the base is subjected to soil uplift pressure. Such tanks usually should be covered to protect the water inside. Designing these tanks requires attention not only to strength requirements, but also to durability and crack control to prevent water leakage and the corrosion of steel reinforcement (ACI 350/350R-06). Therefore, a conservative tank design must be able to withstand applied loads without cracking. Such a design requires a higher reinforcement ratio with adequate bar spacing, greater wall thickness, and high-quality concrete.

Background and Problem Statement

The expansive corrosion of steel reinforcing bars stands out as a significant factor that limits the life expectancy of RC structures. Repairing damage caused by corrosion is a multibillion dollar

problem. RC tanks—among the most important structural facilities in WWTPs—are usually subjected to a uniquely difficult environment in which corrosion poses exceptional challenges. According to the American Water Works Association (AWWA) industry database, the corrosion-related cost of drinking water and sewer systems makes up 75% (\$36 billion) of the annual corrosion costs (\$47.9 billion; NACE International). It includes the cost of replacing aging infrastructure such as RC tanks, lost water from unaccounted-for leaks, and corrosion inhibitors. Concrete tanks deteriorate faster than any other structure because of direct and permanent exposure to aggressive chemical environments (Takeuchi et al. 2004). Yet the need to protect them is often identified only after significant deterioration has occurred. For years, containment designers have tried to achieve crack-free concrete to eliminate the corrosion problem. Techniques have included specific special mix designs, low water-to-cement ratios, many different admixtures, special aggregates, and supplementary cementitious materials, and all have had only limited success. The use of halogens such as chlorine to disinfect drinking water and treat wastewater, as well as ozonation, has a devastating effect on reinforcing steel, regardless of whether it is black, galvanized, or epoxy coated. Chlorine remains the primary oxidant used in chemical treatment, other than oxygen (aeration), and it is considered a corrosive agent in water. Evidently, water must be disinfected and of appropriate quality before being made available to the public. Chloride-induced corrosion of steel reinforcement is very complex and depends on many factors such as chloride concentration, water temperature, and pH. Only by carefully selecting reinforcing materials can the detrimental effects of corrosion be significantly prevented when reinforcement is exposed to aggressive agents. So, the challenge facing structural engineers and municipalities is to design concrete tanks with noncorrosive materials such as fiber-reinforced-polymer (FRP) composite reinforcing bars.

FRP composite bars in general offer many advantages over conventional steel, including one-quarter to one-fifth the density

¹Postdoctoral Fellow, Dept. of Civil Engineering, Univ. of Sherbrooke, 2500 Université Blvd., Sherbrooke, Quebec, Canada J1K 2R1. E-mail: Hamdy.Mohamed@usherbrooke.ca

²NSERC and Canada Research Chair Professor, Innovative Structural FRP Composite Materials for Civil Infrastructure, Dept. of Civil Engineering, Univ. of Sherbrooke, 2500 Université Blvd., Sherbrooke, Quebec, Canada J1K 2R1 (corresponding author). E-mail: Brahim.Benmokrane@usherbrooke.ca

Note. This manuscript was submitted on March 25, 2013; approved on July 26, 2013; published online on October 3, 2013. Discussion period open until March 3, 2014; separate discussions must be submitted for individual papers. This paper is part of the *Journal of Composites for Construction*, © ASCE, ISSN 1090-0268/05013001(11)/\$25.00.

of steel, lack of corrosion even in harsh chemical environments, and greater tensile strength than steel (Benmokrane et al. 2006; 2007; El Salakawy et al. 2003). Since the early 2000s, a joint effort and collaboration between researchers, government organizations, and private industry have been established to develop and implement FRP bars in different applications, primarily focusing on developing and improving glass/carbon composite bars. These developments and improvements, along with numerous successful installations, have led to a much higher comfort level and exponential use of FRP bars by designers and owners. Since glass-FRP (GFRP) bars are more economical than the other available types of FRP bars (carbon and aramid), they have been used extensively in various infrastructure applications such as bridges, parking garages, tunnels, and marine structures [ACI 440R-07 (ACI 2007); Mohamed and Benmokrane 2012]. These field applications and monitoring results have been the basis for validating and improving existing design codes, specifications, and guidelines [i.e., ACI 440.6-08, CSA S807-10 (CSA 2010), CSA-S806-12 (CSA 2012)]. After years of investigation and implementation, public agencies and regulatory authorities in Canada now have included FRP bars as a premium corrosion-resistant reinforcing material in their corrosion-protection policy. That notwithstanding, there have been no implementations reported in the literature to date on the use of FRP bars in WWTP RC tanks to resolve the expansive-corrosion issues to which they are subject.

Objectives

The authors believe that this paper presents the first innovative field application and case study of using FRP bars in a concrete tank for WWTP applications. The objectives of this study are to assess the in-service performance of the FRP-RC tank after several years of operation; to implement FRP bars in RC tanks to overcome the steel expansive-corrosion issues and related deterioration problems; to design durable and maintenance-free concrete for water chlorination tanks used at water treatment plants; and to assess the FRP-design codes and guideline provisions for designing environmentally engineered concrete structures. Moreover, the design and construction details of this tank are used to illustrate code requirements, tank analysis, design details, and construction of FRP-RC tanks.

The following sections describe the tank, FRP materials, design equations, code requirements, construction details, leakage test, monitoring results, and cracking behavior of the FRP-RC walls.

Project Description

The owner and location of the new water treatment plant (WTP) is the town of Thetford Mines in Quebec, Canada. This WTP covers an area of 1,812 m², with a daily treatment capacity of 22,000 m³. The plant's primary water supply is the Grand Lac St.-François. The water is piped from the lake to the plant (approximately 15 km) for treatment. A chlorine disinfection process is used worldwide in WTPs to produce large amounts of safe drinking water as quickly as possible. Water chlorination is the process of adding the element chlorine to water to purify it to make it fit for human consumption. This process is usually performed in a large cistern referred to as a *water chlorination tank*. Thetford Mines decided to use FRP reinforcing bars in the water chlorination tank (see Fig. 1) to extend service life, reduce maintenance costs, avoid the corrosion problem of steel reinforcement, and improve the life-cycle cost efficiency of the new plant. Fig. 1 presents the general overview of the WTP. The tank is considered one of the most important components of the town's new WTP. The tank's structural system is underground, rectangular, resting on rock, and completely buried with compacted fill soil around the walls. The vertical walls support the tank's cover slab and rest on an RC raft foundation. The tank's volume capacity is approximately 2,500 m³, the walls are 4,650 mm high, and the tank measures 24.0 m wide by 23.0 m long. The tank is designed with two closed cells (C_1 and C_2) with a continuous vertical wall (W_M) running down the middle of the tank (see Fig. 1). Each cell is divided to create two zones with a non-continuous interior vertical wall (W_I). The clear spacing between these walls is 5,475 mm. The thicknesses of the exterior and middle walls (W_E and W_M), cover slab, and foundation are all a consistent 350 mm, while the thickness of the interior walls (W_I) is 300 mm.

GFRP Bars

Sand-coated GFRP bars were used to reinforce the tank's three structural elements: the foundation, walls, and cover slab. Two grades of these bars were used: Grade II and III, as classified in

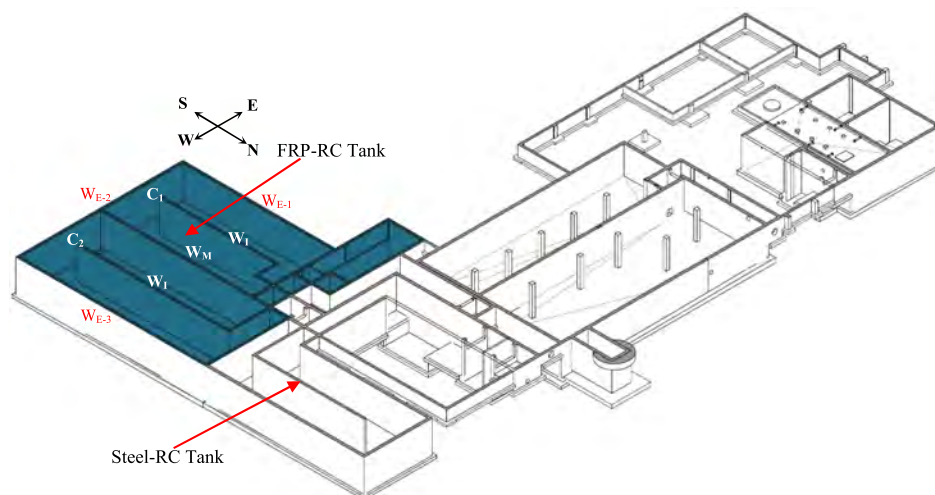


Fig. 1. Overview of the water treatment plant

Table 1. Properties of GFRP Reinforcing Bars Used in the Tank

Bar diameter (mm)	Grade	Guaranteed tensile strength (MPa)	Modulus of elasticity (GPa)	Guaranteed tensile strain (%)
15	II	934	55.4	1.69
15	III	1,105	64.7	1.71
20	III	1,059	62.6	1.69

Note: Data from Pultrall, Inc. (2012).

CAN/CSA S807-10 according to Young's modulus (50 and 60 GPa, respectively). Grade II and III GFRP bars were used in the tank walls, cover slab, and foundation as the secondary and main reinforcements, respectively. Moreover, two bar diameters were used in the tank design: No. 15 and No. 19 (with nominal cross-sectional areas of 199 and 284 mm², respectively, as indicated in CAN/CSA S807-10). Table 1 summarizes the mechanical properties of the GFRP bars, as provided by the manufacturer (Pultrall Inc. 2012).

Tank Design

Codes and Design Equations

The design was made according to CAN/CSA S806-12, (CSA 2012) "Design and construction of building components with fiber-reinforced polymers," and CAN/CSA-A23.3-04 (CSA 2004), "Design of concrete structures." Also, the design was checked to satisfy the requirements of ACI 440.1R-06, "Guide for the design and construction of structural concrete reinforced with FRP bars" and ACI 350/350R-01/06, "Code requirements for environmental engineering concrete structures and commentary". The loads were calculated according to the National Building Code of Canada (NBCC 2005). The tank was designed to determine all the possible loading conditions resulting from water pressure and soil load on the walls and foundation; dead and live loads on the cover slab were considered. According to ACI 350, the full effects of the soil loads and water pressure were considered without the benefit of load resistance, which could minimize the effects of one another. The design involved normal-weight concrete with a target 28-day compressive strength of 35 MPa. The following sections present the summary of the code provisions that were considered in the design.

Flexural Strength

First, the concrete thicknesses of the tank's different structural elements were estimated using the working stress design method based on limiting cracks and concrete tension stress according to ACI 350-06. Thereafter, the limit state design method was used to determine the FRP reinforcement that would satisfy the ultimate design moment ($M_{uDesign}$). The walls, foundation, and cover slab were designed as overreinforced sections as specified by CAN/CSA S806-12 (CSA 2012), considering the following equation:

$$\frac{c}{d} > \frac{7}{7 + 2000\varepsilon_f} \quad (1)$$

FRP reinforcement was used in all the members subjected to combined flexural load, axial compression, and tension force. The FRP reinforcement in the compression zone of the wall was deemed, however, to have zero compressive strength and stiffness (CAN/CSA S806-12). The ultimate design moment ($M_{uDesign}$) on

the walls was calculated considering the applied ultimate flexural moment (M_u) resulting from the soil or water pressure, as well as the axial compressive load (N_u), as follows:

$$M_{uDesign} = N_u(M_u/N_u + 0.5 \times \text{wall thickness} - \text{cover}) \quad (2)$$

Next, the wall's factored moment resistance was determined by taking the moment of tensile and compressive stress resultants about the neutral axis of the concrete cross section as follows:

$$M_r = C_c \left(c - \frac{a}{2} \right) + T_F(d - c) \quad (3)$$

where $C_c = \alpha_1 \phi_c f'_c b a = \alpha_1 \phi_c f'_c b (\beta_1 c)$ (the internal compression force in the concrete block); $T_F = \phi_F \varepsilon_f E_F A_F = \phi_F \{ [\varepsilon_c / c(d - c)] \} A_f$ (the internal tensile forces in the FRP bars)

$$\beta_1 = 0.97 - 0.0025 f'_c \geq 0.67 \quad \alpha_1 = 0.85 - 0.0015 f'_c \geq 0.67$$

Equating the compressive and tensile forces, the value of the neutral axis depth (c) was determined. The ultimate strain at the extreme concrete compression fiber (ε_c) was assumed to be 0.0035 and the resistance factor for GFRP bars (ϕ_F) was taken as 0.75, according to CSA S806-12. All of the tank's structural members were designed such that the factored moment resistance (M_r) was greater than or equal to the effect of $M_{uDesign}$. Then the minimum reinforcement was checked so that $M_r > 1.5M_{cr}$ (CSA S806-12).

Development and Splice Lengths

The development lengths (l_d) of FRP bars at different locations in the tank were verified according to the equation for tension development length in CSA S806-12, as follows:

$$l_d = 1.15 \frac{k_1 k_2 k_3 k_4 k_5}{d_{cs}} \frac{f_f}{\sqrt{f'_c}} A_b \quad (4)$$

Tension development length is a function of the bar diameter (d_d), the design stress in FRP tension reinforcement at the ultimate limit state (f_f), and the specified concrete compressive strength (f'_c). Five other factors affect tension development length: the bar location factor (k_1), concrete density factor (k_2), bar size factor (k_3), bar fiber factor (k_4), and bar surface profile factor (k_5). In the calculation, the corresponding values for these factors were taken to be equal to 1.0, 1.0, 0.8, 1.0, and 1.0, respectively, according to CSA S806-12. Moreover, the calculation of the design stress in the FRP bars at the ultimate limit state (f_f) was simplified to the guaranteed tensile strength of the bars, multiplied by the resistance factor for the GFRP bars ($\phi_F = 0.75$). On the other hand, the design took care to avoid splicing the reinforcement in the tank, although the lengths of the FRP bars in the foundation and cover slab ranged from 9.0 to 16.0 m. Nevertheless, the lap splice length (1,000 mm) at the wall-foundation connection was greater than 1.3 times the development length (l_d) of No. 15 GFRP bars in accordance with CSA S806-12.

Shear Strength

The shear strength was verified according to the type of axial load on the member using the new equations introduced in CAN/CSA S806-12 as follows:

Members subjected to axial tension:

$$V_c = [0.05\lambda_j c k_m k_r (f'_c)^{1/3} b_w d_v] k_s k_a \left(1 - \frac{0.3N_f}{A_g}\right)^3 \geq 0.0 \quad (5)$$

Members subjected to axial compression:

$$V_c = [0.05\lambda_j c k_m k_r (f'_c)^{1/3} b_w d_v] k_s k_a \left(1 - \frac{N_f}{14A_g}\right)^3, \quad \left(1 - \frac{N_f}{14A_g}\right) \leq 3.0 \quad (6)$$

where

$$[0.05\lambda_j c k_m k_r (f'_c)^{1/3} b_w d_v] \geq 0.1\lambda_j c \sqrt{f'_c} b_w d_v$$

$$k_s = \frac{750}{450 + d} \leq 1.0, \quad k_a = \frac{2.5}{M_f / V_f d} \geq 1.0,$$

$$k_m = \sqrt{\frac{V_f d}{M_f}} \leq 1.0, \quad k_r = 1 + (E_F \rho_F)^{1/3}$$

Serviceability and Crack Width Limitation

According to CAN/CSA S806-12, when the maximum strain in FRP tension reinforcement under full service loads exceeds 0.0015, the z value [see Eq. (7)] should be addressed to limit crack width and control stress in the FRP bars. The cross sections of maximum positive and negative moment must be so proportioned that the quantity z does not exceed 45,000 N/mm for interior exposure and 38,000 N/mm for exterior exposure. The numerical limitations for these values correspond to limiting crack widths of 0.7 and 0.5 mm, respectively:

$$z = k_b \frac{E_s}{E_F} f_f \sqrt[3]{d_c A} \quad (7)$$

where $f_f = [M_s / A_f d (1 - k/3)] + (N_s / A_f)$ for members subjected to axial tension (N_s), $f_f = [M_s / A_f d (1 - k/3)] + (N_s / A_f)$ for members subjected to axial compression (N_s), and $k = \sqrt{2\rho_f n_f + (\rho_f n_f)^2} - \rho_f n_f$, $n_f = (E_f / E_c)$, $\rho_f = (A_f / b_w d)$, and $E_c = 4500 \sqrt{f'_c}$

For RC liquid structures reinforced with steel bars, the corresponding z -values according to ACI 350-01 (ACI 2001) are 20,000 and 16,600 N/mm for normal environmental exposure and severe environmental exposure, respectively. The numerical limitations for these values correspond to limiting crack widths of 0.27 and 0.23 mm. These z -values were established for a cover equal to or less than 50 mm. ACI 350-06 has replaced the z factor requirements in the 2001 edition. The maximum allowable stresses now are specified directly as a function of bar spacing as follows:

Normal environmental exposure:

$$20,000 \leq f_{s,\max} = \frac{320}{b \sqrt{s^2 + 4(2 + d_b/2)^2}} \leq 36,000 \text{ psi} (138 \leq f_{s,\max} \leq 248 \text{ MPa}) \quad (8)$$

Severe environmental exposure:

$$17,000 \leq f_{s,\max} = \frac{260}{\beta \sqrt{s^2 + 4(2 + d_b/2)^2}} \leq 36,000 \text{ psi} (117 \leq f_{s,\max} \leq 248 \text{ MPa}) \quad (9)$$

Crack width is inherently subject to wide scatter even in careful laboratory work and is influenced by shrinkage and other time-dependent effects. The best crack control is obtained when the reinforcement is well distributed over the zone of maximum concrete tension (Michaluk et al. 1998; Masmoudi et al. 1996). The current provisions for spacing are intended to limit surface cracks to a width that is generally acceptable in practice but may vary widely in a given structure [ACI 350-06 (ACI 2006)]. The maximum allowable stress (248 MPa) in the steel bar is approximately equal to 60% of the yield strength, which corresponds to 1,240 microstrains. The equivalent stress in the GFRP bar to this strain presents 7% to 8% of its guaranteed tensile strength, according to bar grade (see Table 1). The first attempt at designing this tank was meant to determine the reasonable concrete thickness for controlling the tensile stress in the tension side and hence eliminating the crack. This was achieved by controlling the tensile stresses in the concrete within permissible limits. The tank was designed according to CAN/CSA S806-12 to limit crack and stress, and this led to strain and stress in the FRP bars that was close to the aforementioned stress and strain limitations using ACI 350-01/06. Moreover, using Grade III FRP bars with a small diameter in the design and a less concrete cover optimized the design to a reinforcement ratio that was as close as possible to that needed with steel bars, without going over.

Shrinkage and Temperature Reinforcement

Shrinkage and temperature reinforcement is intended to limit crack width. The stiffness and strength of reinforcing bars control this behavior. Shrinkage cracks perpendicular to the member span are restricted by flexural reinforcement; thus, shrinkage and temperature reinforcement are required only in the direction perpendicular to the span (ACI 440.1R-06). The FRP shrinkage and temperature reinforcement was determined for the walls in the longitudinal direction using the following ACI 440.1R-06 equation:

$$\rho_f = 0.0018 \frac{414 E_s}{f_{fu} E_f} 0.0014 \quad (10)$$

This reinforcement ratio [Eq. (10)] was checked with the minimum reinforcement ratio provided by CSA S806-12, as $\rho_f \geq (400/E_f) A_g$ and $\rho_f \geq 0.0025 A_g$. Moreover, CSA S806-12 and ACI 440.1R-06 limit the spacing of shrinkage and temperature FRP reinforcement to not more than three times the thickness or 300 mm, whichever is less.

Structural Analysis and FRP-Reinforcement Details

The RC tank included walls, a foundation, and a cover slab. The cover slab was designed based on one-way loading action in the short direction, as four statically indeterminate continuous equal spans on a hinged support. Moreover, the loading action on the walls, combined with the foundation, was considered one way in the short direction because the water pressure was resisted by vertical bending moments in the walls. Fig. 2 shows the tank's structural model for the main vertical cross section and the load distribution on each member for a 1.0-m strip width. Each individual member must be capable of resisting the forces acting on it,

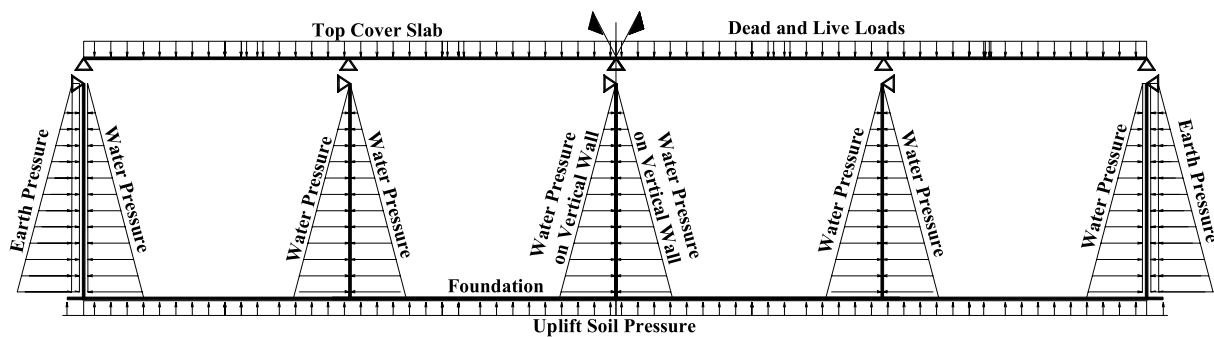


Fig. 2. Structural system and loads on the tank's main vertical section

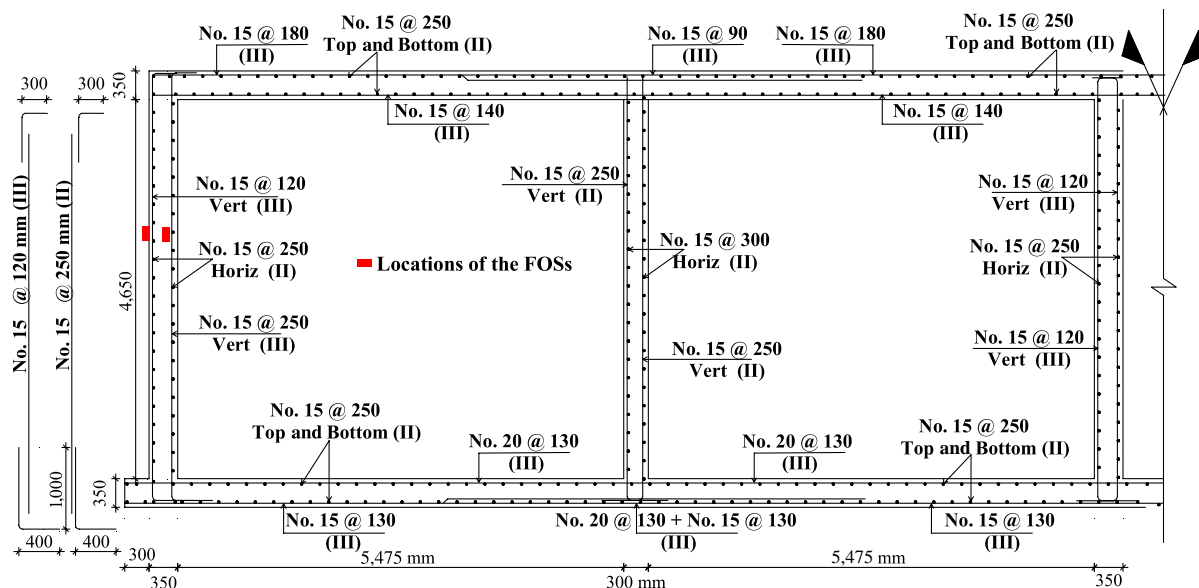


Fig. 3. FRP-reinforcement details for the tank's main vertical section (in mm)

so that the determination of these forces is an essential part of the design process. The bending moments, shearing forces, and axial forces in each member were determined using an elastic-analysis computer program.

Fig. 3 shows a half vertical section of the outer and interior walls, foundation, and cover slab with the axis-symmetric reinforcement details. The tank was designed based on serviceability and the ultimate limit state for FRP reinforcement requirements, while the thickness was determined using the working stress design, as recommended by ACI 350. The moment in the wall varies considerably at different locations. The reinforcing could differ at several locations for a highly efficient design. Wall thickness also could vary, such as either tapering or stepping the wall. For the sake of time, the thickness and reinforcement were kept consistent for the entire wall. One design for the vertical maximum moments was considered to save time for the detailers and construction crew. Usually, crack width must be minimized in tank walls to prevent leakage, as well to minimize the corrosion of steel reinforcement; however, the latter is not an issue with FRP reinforcement. The foundation, wall, and slab thicknesses were determined based on the usual principles, ignoring the tensile strength of concrete in bending. A concrete thickness of 350 mm was chosen for these members and checked to ensure that the tensile stress on the

water-retaining face of the equivalent concrete section did not exceed the permissible tensile strength of concrete. The reinforcement type (steel or FRP bars) does not govern the first estimation of concrete thickness; it depends mainly on concrete strength and service loads. Here, it is of interest to mention that the 350-mm thickness also was used for the tank reinforced with steel bars with the same straining action in the investigated plant. One more benefit of using noncorrosive FRP reinforcing bars in the design is that it makes it possible to reduce the clear concrete cover to 50 mm, as opposed to 60 mm used for the tank reinforced with steel bars.

The size of reinforcing FRP bars was chosen with the knowledge that cracking could be better controlled by using a larger number of small-diameter bars rather than fewer larger-diameter bars (ACI 350). Several bars at moderate spacing are much more effective in controlling cracking than one or two larger bars of equivalent area. For these reasons, No. 15 bars were used extensively in designing the tank, with spacing ranging from 90 to 180 mm. A No. 19 bar, however, was used in only one section of the foundation since the maximum observed moment required a high reinforcement ratio. In designing RC water tanks, it is recommended to use a higher allowable reinforcing bar stress so that fewer bars can be used, resulting in less restraint shrinkage and smaller tensile stresses in the concrete. Hence, the Grade-III GFRP bar with higher

tensile strength and modulus was used as the main reinforcement in the short direction. On the other hand, Grade-II GFRP bar was preferred from a cost-effectiveness point of view for all secondary reinforcements in the tank's long direction. A No. 15 Grade-II GFRP bar was used in the tank in the long direction in the exterior and middle walls, foundation, and cover slab at a spacing of 250 mm. Moreover, this bar was used in the interior walls (W_i) in the short and long directions on both sides, since water pressure acts simultaneously on both faces, resulting in zero moment.

Construction Procedures

The FRP bars were delivered to the site in mid-March. Placement of GFRP reinforcement for the bottom and top foundation mat, as well as concrete casting and curing, were started and finished by the end of March. Continuous plastic chairs were placed in the longitudinal direction at 0.7-m intervals under the bottom reinforcement mat to



Fig. 4. FRP-raft foundation reinforcement

support the FRP bars and maintain the required clear concrete cover. For the top mat, single chairs at 0.9-m intervals in both directions were used. Fig. 4 shows the FRP-reinforcement of the foundation.

Through April and May, the construction on the FRP-RC tank was stopped and shifted to complete and cast the cover slab of the steel-RC tank. Thereafter, wall construction started in May 27, 2012, with the installation of the interior and exterior mats of the FRP reinforcing bars (vertical and horizontal bars). After that, the formwork, casting, and curing of the walls was started and completed on June 5, 2012. Fig. 5 shows the formwork and vertical and horizontal FRP reinforcement of the walls during the different construction stages. The day after the walls were cast, all the formwork for the interior walls on both sides was removed, while the exterior formwork for the outer walls was maintained and used through all the construction stages of the cover slab. The formwork for the cover slab started directly after removing the wall formwork and was finished in mid-June. The placement of GFRP reinforcement for the bottom and top mats of the cover slab and concrete casting was finished by June 22, 2012. In addition, continuous plastic chairs were placed in the longitudinal direction at 0.8-m intervals under the bottom of the top reinforcement mat to support the FRP bars and maintain the required clear concrete cover. Fig. 6 shows the FRP reinforcement in the cover slab before and during casting. After casting, the slab was cured for 10 days, with the formwork being completely removed 4 days later. Following that, cleaning and leveling of the top surface of the foundation with cement mortar were completed in mid-July so that the tank could be filled with water.

Water stops were used in this tank at the wall-foundation connection for the interior and exterior walls. Moreover, vertical expansion joints were introduced between the walls of the steel and FRP tanks. In conclusion, under these difficult working conditions,



Fig. 5. Wall construction details: (a) formwork, vertical and horizontal FRP reinforcements before casting the walls; (b) using bent FRP bars at the corner; (c) walls after casting



Fig. 6. Overview of cover slab: (a) formwork and FRP reinforcements; and (b) during casting

all the construction stages of the tank, starting from the foundation and walls and finishing with the cover slab, were completed with no additional precautions about the concrete casting or the handling and placement of the GFRP bars compared to steel. The construction and installation practices required when using FRP reinforcing bars were similar to those used with steel bars in the FRP and steel tanks, respectively. The construction crews reacted positively, indicating that more FRP bars could be handled and placed in formwork in less time due to their light weight. The FRP bars did not move or float during concrete placement and vibration, and they withstood all on-site handling and placement with no problems.

Wall Instrumentation

The FRP-RC tank was instrumented at critical locations to measure internal strain data using Fabry-Perot fiber-optic sensors (FOSs) (Roctest 2012). The objective of using FOSs was to allow for the long-term monitoring of the tank. The wall and cover slab were instrumented at different locations with 6 and 10 FOSs, respectively. In this paper, only strain data and crack behavior of the vertical walls are presented. One of the tank's exterior walls was chosen to be instrumented to collect strain data at the maximum moment location for the two loading conditions: water and soil pressure. Three FOSs were glued to three vertical GFRP reinforcing bars on each side of the wall (on the interior and exterior mats). The GFRP bars were instrumented at the structural laboratory at the University of Sherbrooke. Thereafter, the bars were shipped to the construction site, where they were installed at the designated location during the wall's construction stage. The interior and middle walls were not instrumented, since the water pressure acts on both sides. It is of interest to mention that an FOS can measure strain data in the range of positive and negative 3,500 microstrains. The benefit of doing this lies with collecting the tensile and compressive strains in the FRP bars since, in the case of the exterior wall, the moment is reversible due to the opposing effects of soil and water pressure.

Water Leakage Test

The leakage test was performed three days immediately after the removal of the cover slab's formwork and before any backfilling. The steel-RC and FRP-RC tanks were tested by the contractor and witnessed by the consulting engineer. As mentioned previously, the tank had two cells, so each cell should be considered a single tank and tested individually. One of these cells was filled completely with water to check for leakage; the other cell remained empty. After finishing the test on one side of the tank and checking for all visible cracks, the water was transferred to the other cell.



Fig. 7. Overview of the completed tank during the leakage test, prior to backfilling

Fig. 7 shows the tank overview during the leakage test of one cell. The water was kept at the testing level for three days prior to the actual test. The tank's exterior wall surfaces were inspected while the tank was being filled.

Flexural Cracks

Visual inspection of the tank over three days indicated that the leakage test did not induce flexural horizontal cracks in all the walls. No water leakage was observed, which would indicate flexural crack leaking. This can be attributed to the compression zone developed in one side of the wall section as the result of flexural stresses, which could effectively prevent leakage through cracks regardless of the crack widths. At this juncture, it is of interest to mention that the cracking moment strength for the 350-mm-thick wall is $75 \text{ kN} \cdot \text{m/m}$. This moment is almost greater than the service moment in the wall resulting from the water pressure. The walls were designed to minimize the crack width resulting from the one-way loading action of the water pressure in the vertical direction. This means that the flexural cracks are not of concern with regard to leakage because the liquid passage through the depth of the section is obstructed by the presence of uncracked concrete in the compression zone. Nevertheless, the compression zone depth should be controlled to limit liquid loss through concrete permeability. This result is consistent and in good agreement with the research work and experimental test results conducted by Ziari and Kianoush (2009).

Shrinkage and Restraint Cracks

During the leakage test, a site inspection showed that the water tank developed limited vertical shrinkage cracks, which became leaks

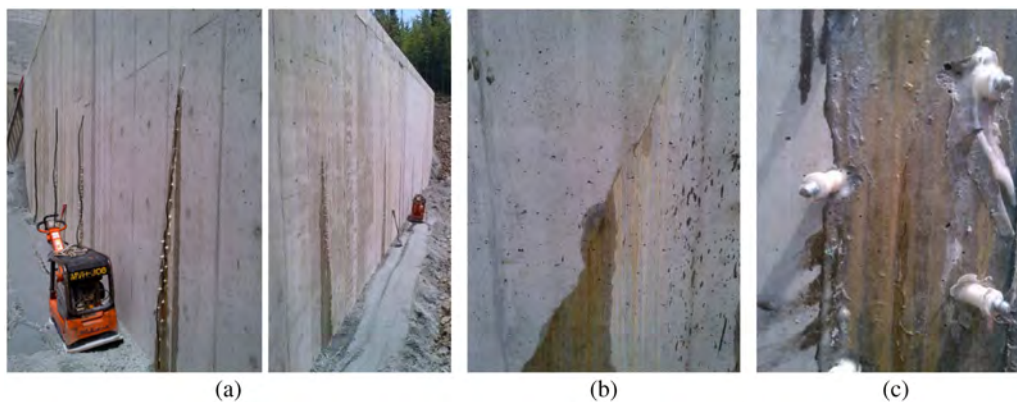


Fig. 8. Overview of the general cracking behavior during the leakage test on the FRP-RC tank: (a) crack patterns in the exterior walls during the leakage test; (b) inclined crack at the corner; (c) injection ports and crack injection

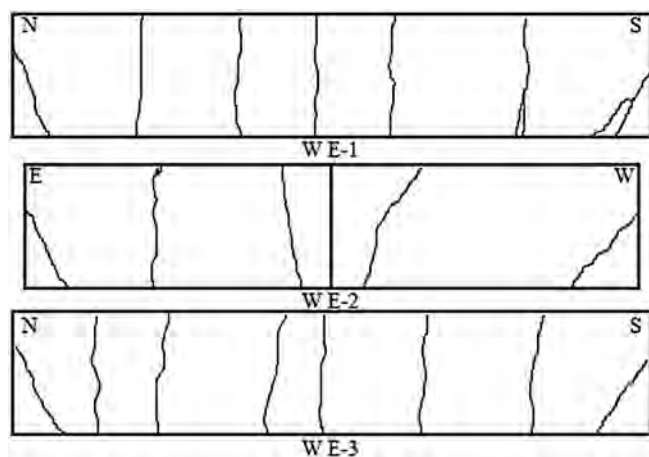


Fig. 9. Schematic crack patterns resulting from restrained early thermal contraction and autogenous shrinkage for the three FRP-RC walls

that did not self-seal. Figs. 8(a and b) show the crack patterns through one of the exterior walls (W_{E-1}). Such cracks are common and expected in the liquid tank at the first stage of service loading. These are minor indications and have no real structural impact on the tank. Controlling leakage means that, while cracks cannot be prevented, they must be minimized, and crack width should be kept below a certain limit under service loads (Ziari and Kianoush 2009). The leakage test results for the FRP tank indicated that

the number of observed cracks in the exterior surfaces of walls W_{E-1} , W_{E-2} , and W_{E-3} were 7, 5, and 8, respectively (see Fig. 9). The cracks were perpendicular to the direction of the maximum principal stress induced by moment. The cracks extended from the base and propagated up to the full height of the wall. One inclined crack in each wall was observed at the corner of the tank, propagating from the base toward the corner edge at an angle of about 45° . This crack stopped below the mid-height of the wall. The engineer described the observed cracks as “minor” leaks, as was expected for this structure. The crack width was measured using a handheld microscope, with the measured widths ranging from 0.06 to 0.18 mm, which is less than the allowable limit (ACI 350). On the other hand, the leakage test had been conducted for the steel-RC tank one month earlier. Despite the fact that the shrinkage reinforcement used in the steel-RC tank was higher than that used in the FRP tank (a No. 15 steel bar at 225 mm on both sides, versus a No. 15 GFRP bar at 250 mm on both sides). The leakage test results for the steel tank, however, indicated that the number and widths of the observed cracks in the exterior surfaces for similar wall dimensions were insignificantly higher than that observed in the FRP-RC tank. The measured crack widths ranged from 0.097 to 0.24 mm. Fig. 10 shows the crack patterns through one of the exterior walls for the steel-RC tank and presents the leakage with an indication of the initiation of corrosion of internal steel reinforcement. The following section presents a summary and explanation for the tank’s crack behavior.

In general, the problem of cracking in concrete results from its low tensile strength. Once the concrete’s tensile strength is



Fig. 10. Overview of the general cracking behavior during the leakage test on the steel-RC tank: (a) crack patterns in the exterior wall; (b) close up view of the crack

exceeded, a crack will develop. The number and width of the cracks that develop are influenced by the amount of shrinkage that occurs, the restrained volumetric deformations, and the amount and spacing of reinforcement provided [ACI 209R-92 (ACI 1997)]. Plastic-shrinkage cracking is a problem for large flat structures, such as the cover slab and the vertical walls of this water tank, in which the exposed surface area is high relative to the volume of the placed concrete. Plastic-shrinkage cracks are immediately apparent, visible within 0 to 2 days of placement, while drying-shrinkage cracks develop over time (Bamforth 2007). Restraint in the concrete wall of the tank is provided externally from the continuous restraint along the edge connection with foundation, and internally by differential drying shrinkage and FRP reinforcement. The schematic cracking pattern due to continuous edge restraint of the three FRP-RC walls is shown in Fig. 9. This was where the foundation of the tank restrained the early thermal movements of the wall that had been cast later. Without restraint, the section would have contracted along the line of the base. Therefore, the restraint allows a horizontal force to develop, which led to vertical full-section cracking. The restrained thermal strain at early age varied from zero from the base up to a maximum strain adjacent to the base. When a tank is filled with water, the tension in the walls causes an extension of the tank walls. This behavior is restrained at the base so that the imposed strains reduce to a negligible level adjacent to the base. As each crack forms, the propagation of that crack to the full height of the wall will cause a redistribution of base restraint such that each portion of the wall will act as an individual section between cracks. Prior to cracking, the stress in the longitudinal reinforcement of the wall subjected to shrinkage depends primarily on the differences in coefficients of thermal expansion between the reinforcement (FRP or steel) and concrete. When the coefficients are equal, the reinforcement becomes stressed as crack propagation reaches the reinforcement. The average coefficients of thermal expansion of concrete and steel are approximately 8×10^{-6} and $12 \times 10^{-6}/^{\circ}\text{C}$, respectively, while the GFRP bars used in the design have a coefficient of thermal expansion $7 \times 10^{-6}/^{\circ}\text{C}$. So, the coefficient of thermal expansion of the GFRP bars used is close to that of concrete, eliminating large internal stresses due to differences in thermal expansion or contraction, thereby preventing any adverse effect.

The previously discussed cracking pattern is independent of the amount of reinforcement used in the concrete wall. Cracking behavior can be controlled only by providing an appropriate area of distribution reinforcement. When sufficient reinforcement is provided to achieve the critical reinforcement ratio, the widths of these primary cracks are controlled, although secondary cracks may be induced. Cracking extent and size will then depend on the amount and distribution of reinforcement provided. The role of reinforcement is to redistribute stresses after the formation of each crack [ACI 224R-01 (ACI 2001)]. A higher reinforcement ratio results in the formation of a higher number of cracks, thereby reducing crack width. This could be the reason for the observed number of cracks in the FRP-RC tank, which were fewer than in the steel-RC tank. Previous research work has shown that, for an unreinforced concrete wall, full-section restraint cracks can be spaced in the neighborhood of 1.0 to 2.0 times the height of the wall. The leakage test results showed that the crack spacing ranged from 0.6 to 0.75 and from 0.5 to 0.65 times the height of the wall in the FRP-RC and steel-RC tanks, respectively. This is attributed to the shrinkage reinforcement used to control crack width; hence, more cracks were observed. On the other hand, it was noticed that the maximum crack width resulting during the leakage test did not occur at the wall base, but at a distance of about 0.25 to 0.3H from the joint (where H is the wall height).



Fig. 11. Overview of the tank completely buried, with compacted fill soil around the walls and 600 mm over the cover slab, FOS PVC box, and strain-data capture

This is because the restraint from the base prevented the cracks from opening locally to the joint. Crack-width limitations are recommended by ACI 350-01 specifically for flexural cracks in environmental-engineering concrete structures. According to this code, flexural-crack widths should be limited to 0.23 and 0.27 mm for severe and normal environmental exposures, respectively. It is not clear, however, which type of crack is considered in this design guideline. Moreover, ACI 350 provides the minimum shrinkage reinforcement ratio that should be used in the longitudinal direction based on the grade of steel bars. The shrinkage reinforcement in the FRP-RC walls was designed and controlled according to the provisions of CAN/CSA S806-12 and ACI 440.1R-06, in terms of limits, spacing, and required reinforcement ratio. A No. 15 GFRP bar at 250 mm on both sides with a reinforcement ratio equal to 0.0045 was used (0.00225 each side). The leakage-test results indicated that using S806-12 and ACI 440.1R-06 limited the number of cracks and controlled crack widths to reasonable values.

After completing the leakage test for each tank cell, it was decided to repair the cracks causing the leaks with an external injection system in each wall. Crack injection has been performed for many years. The injection procedure would entirely fill the crack, from front to back. Injection has proved to be effective for filling cracks from 0.002 to 50 mm in width. All the cracks were repaired using pressure injection of polyurethane foam sealant after inserting the stainless-steel injection ports around the cracks in the vertical direction. Figs. 8(c and d) show crack leaking, stainless-steel injection ports and foam sealant over the crack. This material is water activated for use in wet environments, so there was no need to empty the tank. The injection sealant continues to work for considerable time after application. So, if there is future movement, the sealant will expand and contract to compensate for it. After treatment, the leaking stopped and the wall started to dry out. Thereafter, the construction work for the backfill was started immediately after ensuring that there was no leakage. The exterior walls were buried with compacted fill soil; a vibratory-plate compactor was used for compaction. The surface area of the cover slab was buried under 600 mm of uncompacted fill soil (see Fig. 11). Finally, water was pumped from the lake to the WTP on November 6, 2012.

Wall Tensile- and Compressive-Strain Measurements

Fig. 12 shows the strain measurements from the FOSs attached to the GFRP bars for interior and exterior vertical reinforcement.

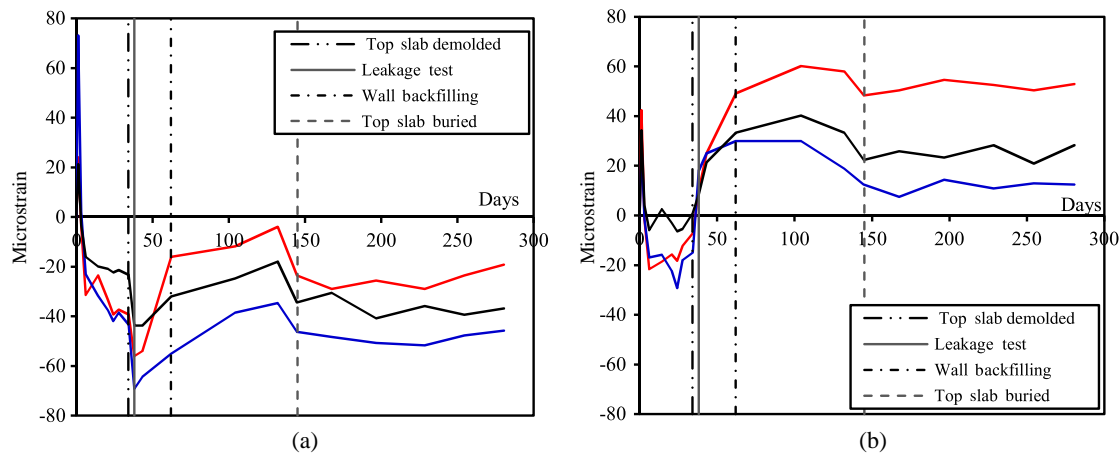


Fig. 12. Measured strains in the vertical FRP reinforcement in the wall (W_{E-1}): (a) interior reinforcements; (b) exterior reinforcements

The initial strain readings were recorded a few hours before casting (zero point at the x -axis). After casting, the strain readings were recorded daily for one week. Following that, the six wall FOSs were monitored each week. Therefore, the reported strain values in the first 10 days represented concrete shrinkage. Moreover, the high temperature due to cement hydration at early age could be observed. Fig. 12(a) shows that the maximum recorded compressive strain ranged from 40 to 70 microstrains during the leakage test. The recorded strain values resulted from water pressure, cover-slab dead weight, and the wall itself. In addition, Fig. 12(b) shows the sudden variation from compressive to tensile strain, as a result of the wall moment due to water pressure. The maximum tensile strain ranged from 40 to 60 microstrains during the leakage test and after the backfilling was initiated. The measured values indicate that the strains in the wall were insignificant, as they represented less than 1.0% of the ultimate strain of the GFRP bars. This can be attributed to two reasons. First, considering the straining action of these forces and determining the maximum compressive and tensile stresses on the wall, the results will be approximately equal to -0.8 and 0.5 MPa, respectively. These values are insignificant compared to the strength capacity of the wall cross section. On the other hand, the cracking moment of the wall's cross section is higher than that the actual moment during the leakage test. This was confirmed from the site inspection during the leakage test since no flexural cracks were observed. The backfilling work started immediately after the shrinkage cracks were repaired, making it possible to release the water pressure given the opposing action of soil pressure. Nevertheless, the strain in the GFRP bars in the exterior mat continued to increase up to the addition of uncompacted soil over the cover slab. Beyond that, the compressive strain increased insignificantly as a result of the dead load from the soil fill. On the other hand, the tensile strain decreased and stabilized as the result of the opposing action of the water and soil pressures, in addition to the soil's weight on the cover slab. In conclusion, the captured strain values are insignificant compared to the allowable stress of the tank's service design load.

Conclusions

This paper presents the design procedures, construction details, leakage testing, and monitoring results for the world's first RC water chlorination tank that is totally reinforced with GFRP bars. Based on the construction details, the results of the leakage test,

and strain data captured under service conditions, the following conclusions can be drawn:

- The GFRP bars provided an efficient way to overcome the expansive steel-corrosion issues and related deterioration problems in the water chlorination tank.
- The design provisions used in the water chlorination tank showed that the proposed reinforcement ratios adopted by building codes and guidelines (CAN/CSA S806-12; ACI 440.1R-06, and ACI 350/350R-06) are adequate to meet serviceability and strength criteria.
- No obstacles to construction resulting from the GFRP bars were encountered throughout the tank's construction. The GFRP bars withstood normal on-site handling and placement with no problems.
- The FRP-RC water tank performed very well and was able to withstand the applied loads or leaking during the leakage test. The GFRP reinforced-concrete walls, foundation, and slab showed normal structural performance in terms of strain and cracking throughout 10 months of real service conditions.
- The cost-effectiveness of using GFRP bars in the tank was optimized by using Grades II and III in the longitudinal and transverse directions, respectively, and by using a small bar diameter rather than using a larger diameter with smaller spacing.
- Finally, this successful field application demonstrated the effective use of GFRP bars in an RC tank for a water treatment plant for the first time. The structural performance of this first application of its type and scale, based on the monitoring and continuous observations, was anticipated. This application opens the door to a major application of FRP reinforcing bars in RC water tanks in North America and across the world. RC water tanks with GFRP bars would extend the life of such structures to 100 years or more compared to steel-RC tanks, which needs major restoration after 25 years.

Acknowledgments

The authors would like to thank and express their sincere appreciation to the Natural Science and Engineering Research Council of Canada (NSERC), Canada Research Chair in Advanced Composite Materials for Civil Structures and NSERC/Industry Research Chair in Innovative FRP Reinforcement for Concrete Infrastructure, in the Department of Civil Engineering, Faculty of Engineering, University of Sherbrooke, Quebec, Canada, the Fonds de recherche québécois en nature et technologies (FRQ-NT), Roche Consulting

Engineers (Thetford Mines, Quebec, Canada), the general contractor Wilfrid Allen Company (Thetford Mines, Quebec, Canada), and the Engineering Services of the City of Thetford Mines (Quebec, Canada).

Notation

The following symbols are used in this paper:

- A = effective tensile area of concrete surrounding the flexural tensile reinforcement and extending from the extreme tensile fiber to the centroid of the flexural tensile reinforcement and an equal distance past the centroid, divided by the number of bars;
- A_b = area of an individual bar (mm^2);
- A_F = area of FRP reinforcement (mm^2);
- A_g = gross area of section;
- b_w = minimum effective web width (mm);
- c = neutral-axis depth (mm);
- c_b = neutral-axis depth at the balanced strain condition (mm);
- d = effective depth (mm);
- d_b = bar diameter (mm);
- d_c = thickness of the cover from the tensile face to the center of the closest bar (mm);
- d_v = effective shear depth, taken as the greater of $0.9d$ or $0.72h$;
- E_c = modulus of elasticity of concrete (MPa);
- E_F = modulus of elasticity of FRP (MPa);
- E_s = modulus of elasticity of steel reinforcement;
- f_{Fu} = ultimate tensile strength of FRP (MPa);
- f_F = tensile stress in FRP reinforcement;
- f_s = tensile stress in steel reinforcement;
- f'_c = concrete compressive strength (MPa);
- f_{cr} = cracking strength of the concrete (MPa);
- I_{cr} = cracking moment of inertia (mm^4);
- I_e = effective moment of inertia (mm^4);
- I_g = gross moment of inertia (mm^4);
- k_a = coefficient taking into account the effect of arch action on member shear strength;
- k_b = coefficient dependent on the reinforcing-bar bond characteristics;
- k_m = coefficient taking into account the effect of moment at section on shear strength;
- k_s = coefficient taking into account the effect of member size on its shear strength;
- k_r = coefficient taking into account the effect of reinforcement rigidity on its shear strength;
- M_{cr} = cracking moment ($\text{kN} \cdot \text{m}$);
- M_f = factored moment ($\text{kN} \cdot \text{m}$);
- M_r = factored moment resistance ($\text{kN} \cdot \text{m}$);
- M_s = service moment ($\text{kN} \cdot \text{m}$);
- N_f = factored axial load normal to the cross-section occurring simultaneously with V_f , including effects of tension due to creep and shrinkage (taken as positive for tension and negative for compression);
- N_s = service axial load normal to the cross section;
- n_f = ratio of modulus of elasticity of FRP bars to modulus of elasticity of concrete;
- s = bar spacing (mm);
- V_c = factored shear resistance provided by the concrete (kN);
- β_1 = ratio of depth of equivalent rectangular stress block to depth of the neutral axis;
- ϵ_c = maximum concrete compressive strain;
- ϵ_F = maximum tensile strain of FRP bars (%);
- λ = factor to account for concrete density;

- ρ_F = longitudinal FRP reinforcement ratio; and
- ϕ_c = resistance factor for concrete.

References

- American Concrete Institute (ACI). (2001). "Control of cracking in concrete structures." *ACI 224R-01*, Farmington Hills, MI.
- American Concrete Institute (ACI) Committee 209. (1997). "Prediction of creep, shrinkage and temperature effects in concrete structures." *ACI 209R-92*, Farmington Hills, MI.
- American Concrete Institute (ACI) Committee 350. (2001). "Code requirements for environmental engineering concrete structures and commentary." *ACI 350*, Farmington Hills, MI.
- American Concrete Institute (ACI) Committee 350. (2006). "Code requirements for environmental engineering concrete structures and commentary." *ACI 350*, Farmington Hills, MI.
- American Concrete Institute (ACI) Committee 440. (2006). "Guide for the design and construction of concrete reinforced with FRP bars." *ACI 440.1R-06*, Farmington Hills, MI.
- American Concrete Institute (ACI) Committee 440. (2007). "Report on fiber-reinforced polymer (FRP) reinforcement for concrete structures." *ACI 440R-07*, Farmington Hills, MI.
- Bamforth, P. B. (2007). "Early-age thermal crack control in concrete." *CIRIA C660*, CIRIA, London.
- Benmokrane, B., El-Salakawy, E., El-Ragaby, A., and Lackey, T. (2006). "Designing and testing of concrete bridge decks reinforced with glass FRP bars." *J. Bridge Eng.*, 11(2), 217–229.
- Benmokrane, B., El-Salakawy, E., El-Ragaby, A., and El-Gamal, S. (2007). "Performance evaluation of innovative concrete bridge deck slabs reinforced with fibre-reinforced polymer bars." *Can. J. Civ. Eng.*, 34(3), 298–310.
- Canadian Standards Association (CSA). (2010). *CAN/CSA S807-10, Specification for fibre-reinforced polymers*. Rexdale, Ontario, Canada.
- Canadian Standards Association (CSA). (2012). "Design and construction of building components with fiber reinforced polymers." *CAN/CSA S806-12*, Rexdale, Toronto.
- Canadian Standards Association (CSA) Technical Committee on Reinforced Concrete Design. (2004). "Design of concrete structures." *A23.3-04*, Rexdale, Toronto.
- El-Salakawy, E., Benmokrane, B., and Desgagné, G. (2003). "FRP composite bars for the concrete deck slab of Wotton Bridge." *Can. J. Civ. Eng.*, 30(5), 861–870.
- Masmoudi, R., Benmokrane, B., and Chaallal, O. (1996). "Cracking behaviour of concrete beams reinforced with fiber reinforced plastic rebars." *Can. J. Civ. Eng.*, 23(6), 1172–1179.
- Mohamed, H. M., and Benmokrane, B. (2012). "Recent field applications of FRP composite reinforcing bars in civil engineering infrastructures." *Proc. Int. Conf. ACUN6-Composites and Nanocomposites in Civil, Off-shore, and Mining Infrastructure*, Nov. 14–16, 2012, Monash Univ., Melbourne, Australia.
- Michaluk, C. R., Rizkalla, S. H., Tadros, G., and Benmokrane, B. (1998). "Flexural behavior of one-way concrete slabs reinforced by fiber-reinforced plastic reinforcements." *ACI Struct. J.*, 95(3), 353–365.
- NACE International. "Corrosion costs and preventive strategies in the United States." *Publication No. FHWA-RD-01-156*, National Association for Corrosion Engineers, Houston, TX.
- National Building Code of Canada (NBCC). (2005), National Research Council, Ottawa, ON.
- Pultrall, Inc. (2012). "Composite reinforcing rods technical data sheet, Thetford Mines, Canada." (www.pultrall.com) (Jan. 12, 2012).
- Roctest Ltd.. (2012). "Integrated instrumentation and structural health monitoring solution." Saint-Lambert, QC, Canada (www.roctest-group.com).
- Takeuchi, H., Taketomi, S., Samukawa, S., and Nanni, A. (2004). "Renovation of concrete water tank in Chiba Prefecture, Japan." *Pract. Period. Struct. Des. Constr.*, 10.1061/(ASCE)1084-0680(2004)9:4(237), 237–241.
- Ziari, A. M., and Kianoush, R. (2009). "Investigation of flexural cracking and leakage in RC liquid containing structures." *Eng. Struct.*, 31(5), 1056–1067.